

Past seismic slip-to-the-trench recorded in Central America megathrust

Paola Vannucchi^{1,2*}, Elena Spagnuolo³, Stefano Aretusini⁴, Giulio Di Toro^{5,6}, Kohtaro Ujiie⁶, Akito Tsutsumi⁷ and Stefan Nielsen⁸

The 2011 Tōhoku-Oki earthquake revealed that co-seismic displacement along the plate boundary megathrust can propagate to the trench. Co-seismic slip to the trench amplifies hazards at subduction zones, so its historical occurrence should also be investigated globally. Here we combine structural and experimental analyses of core samples taken offshore from southeastern Costa Rica as part of the Integrated Ocean Drilling Program (IODP) Expedition 344, with three-dimensional seismic reflection images of the subduction zone. We document a geologic record of past co-seismic slip to the trench. The core passed through a less than 1.9-million-year-old megathrust frontal ramp that superimposes older Miocene biogenic oozes onto late Miocene-Pleistocene silty clays. This, together with our stratigraphic analyses and geophysical images, constrains the position of the basal decollement to lie within the biogenic oozes. Our friction experiments show that, when wet, silty clays and biogenic oozes are both slip-weakening at sub-seismic and seismic slip velocities. Oozes are stronger than silty clays at slip velocities of less than or equal to 0.01 m s^{-1} , and wet oozes become as weak as silty clays only at a slip velocity of 1 m s^{-1} . We therefore suggest that the geological structures found offshore from Costa Rica were deformed during seismic slip-to-the-trench events. During slower aseismic creep, deformation would have preferentially localized within the silty clays.

Geodetic data, seafloor bathymetry and tsunami inversion modelling all indicate that the 2011 M_w 9 Tōhoku-Oki earthquake ruptured to the trench, with 50–80 m co-seismic slip occurring across the shallow portion of the megathrust^{1–3}. These exceptional data sets showed, for the first time, that ruptures can propagate to the trench during subduction megathrust earthquakes. Previously, this domain had been considered to slip only aseismically⁴. This observation immediately raises follow-on questions: Is there evidence that co-seismic slip to the trench has occurred in other subduction zones? What is the potential for other megathrusts to co-seismically rupture to the trench?

Following ocean drilling results in the Japan Trench⁵, investigation has focused on the smectite-rich, pelagic clays recovered from the shallow portions of the Tōhoku megathrust. Friction experiments showed that when the fault's original fabric is preserved, the Tōhoku pelagic clays are cohesionless, reducing fracture energy and favouring earthquake rupture propagation⁶. The very small fracture energy and shear stress of pelagic clays when sheared at seismic slip velocities ($\sim 1\text{ m s}^{-1}$) can allow propagation of earthquake rupture from depth^{7,8}, explaining slip to the trench during the 2011 Tōhoku-Oki earthquake⁸. On the ocean floor, deposition of pelagic sediments typically alternates between clays and biogenic oozes^{9,10}, with the latter mostly subducting in the eastern central and south Pacific (Fig. 1). In contrast to pelagic clays, biogenic oozes have been proposed to inhibit both fault rupture propagation and displacement during earthquakes, and so prevent the occurrence of tsunamis⁹. Laboratory friction experiments have suggested, however, that biogenic oozes may play a key role in earthquake nucleation at depth^{11–13}.

In this study, we report evidence from ocean drilling in southern Costa Rica that biogenic oozes are the host sediment for the decollement at the trench. This observation, combined with the result from high-velocity friction experiments, suggests that near-trench slip here was rapid, and probably tsunamigenic.

Basal decollement location offshore southeast Costa Rica

Studies of the shallower extents of subduction megathrusts have relied heavily on ocean drilling; only modern subduction systems offer a clear view of frontal prism geometry and the in situ properties of the material involved in the fault zone. Integrated Ocean Drilling Program Expedition (Exp.) 334 and Exp. 344, the Costa Rica Seismogenesis Project (CRISP), targeted both the incoming Cocos Plate sedimentary section at IODP Sites U1381 and U1414, and the frontal prism at Site U1412, the latter located $\sim 3\text{ km}$ landward of the Middle America Trench axis (Fig. 2, insets A and B). The incoming plate sedimentary succession consists of Miocene pelagic biogenic oozes overlain by late Miocene to Pleistocene hemipelagic silty clays (Fig. 2, inset C). At Site U1381, the oozes directly lie on Cocos Ridge basalt, while at Site U1414, a well-lithified layer of sandstone is interposed between the oozes and this basalt (Fig. 2, inset C). Here, the thickness of the incoming plate sediment section varies considerably both along-strike and downdip because of the rugged topography of the Cocos Ridge. Moving toward the frontal prism, reflection seismic profiles show a 5–10-km-wide frontal accretionary prism¹⁴ (Fig. 2, inset A). The portion of the frontal prism drilled during IODP Exp. 344 at Site U1412 consists of Miocene pelagic biogenic oozes overlain by late Miocene to Pleistocene hemipelagic silty clays, both resting on top of younger Pleistocene silty clays (Fig. 2, inset B). This stratigraphy implies that the frontal prism is indeed

¹Department of Earth Sciences, Royal Holloway, University of London, Egham, UK. ²Dipartimento di Scienze della Terra Università di Firenze, Firenze, Italy. ³Sezione di Sismologia e Tettonofisica, Istituto Nazionale di Geofisica e Vulcanologia, Roma, Italy. ⁴School of Earth, Atmospheric and Environmental Sciences, Manchester University, Manchester, UK. ⁵Dipartimento di Geoscienze, Università di Padova, Padova, Italy. ⁶Department of Geosciences, University of Tsukuba, Tsukuba, Japan. ⁷Graduate School of Science, Kyoto University, Kyoto, Japan. ⁸Department of Earth Sciences, University of Durham, Durham, UK. *e-mail: paola.vannucchi@rhul.ac.uk

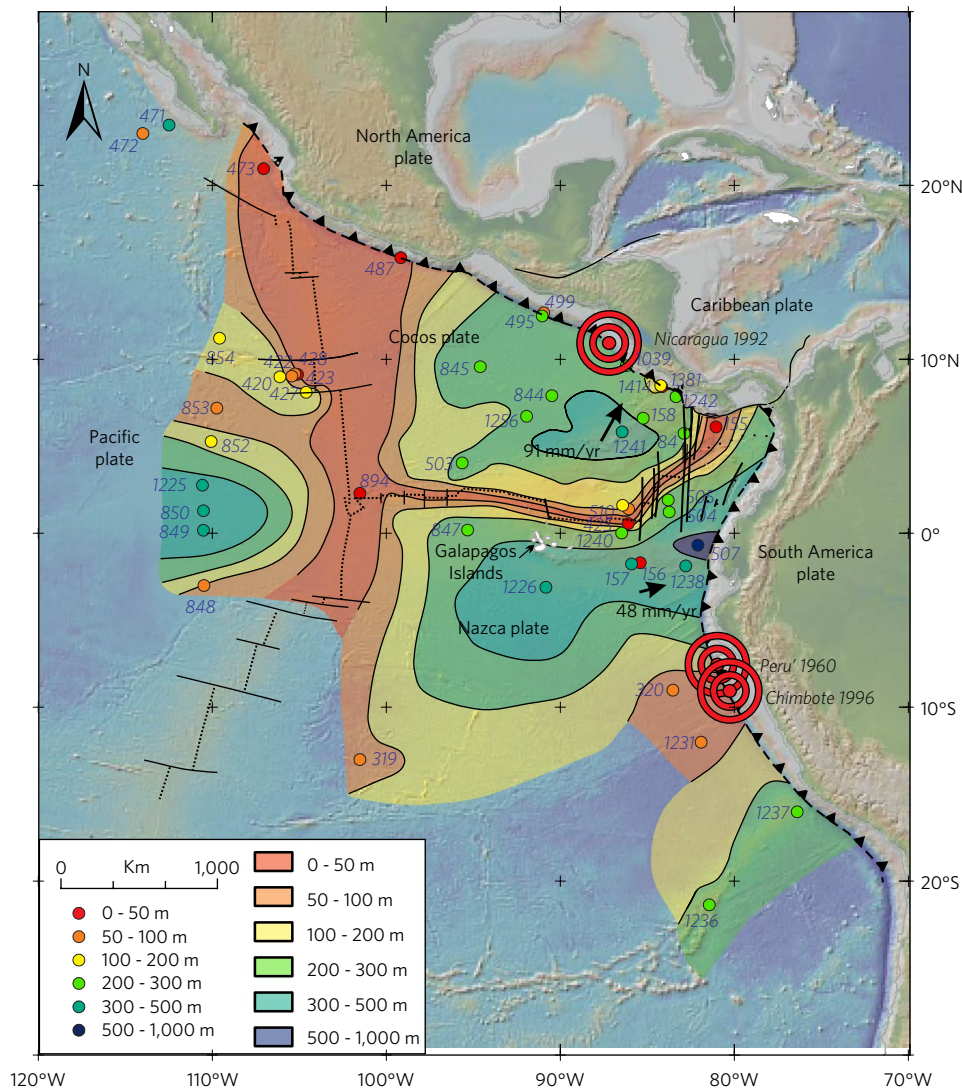


Fig. 1 | Distribution and thickness of biogenic oozes (mostly carbonaceous) on the Cocos and Nazca plates as calculated by DSDP-ODP-IODP drilling results. The blue numbers next to the circles indicate the DSDP-ODP-IODP drilling site used for the isopach map. Note that our interpolation does not consider bathymetry variations.

formed by oceanic sediments scraped off from the incoming plate and accreted through a series of thrusts at the front of the subduction margin (Fig. 2, inset C). Most importantly, although Site U1412 did not reach the modern basal decollement, it drilled through a former frontal thrust. The thrust occurs between ≈ 321 and ≈ 329 mbsf, at the base of ≈ 120 m biogenic oozes. Although the actual thrust surface was not recovered, the core catcher of Core 344-U1412C-4R contained mixed Miocene and Pleistocene sediments, with no traces of the lithological units below the biogenic oozes.

This thrust is the ramp of a thrust system in which the biogenic oozes form the hangingwall. These are the youngest possible sediments that could be cut by the basal decollement, which means that the decollement propagated neither in the silty clays nor along the silty clay/biogenic ooze boundary. High-resolution three-dimensional seismic reflection data¹⁵ show ≈ 125 -m-thick underthrust sediments landward of Site U1414, where drilling shows the total thickness of the biogenic oozes is ≈ 180 m. This argues against the possibility that the basal decollement follows the basalt/oozes boundary.

The lack of seafloor crests and clear offsets to the lower slope deposits landward of the frontal thrust (Fig. 2, inset A) supports the

hypothesis of an imbricate stack of thrust sheets in which the frontal thrust remains active until a new frontal thrust forms seaward of it. The basal decollement propagates in the direction of slip along a weak surface, and near the toe it can ramp up-section. Although Site U1412 did not reach the modern decollement, both the presence of this old frontal thrust and three-dimensional seismic reflection imaging imply that biogenic oozes were the layer in which the megathrust propagated—that is, the basal decollement—beneath this accretionary prism (Fig. 2, inset B).

Sample material and in situ conditions

The biogenic oozes are formed by various proportions of calcareous nanofossils, planktonic and benthonic foraminifera, radiolarians, diatoms and sponge spicules. The average mineralogical composition of our samples is 80% calcite and 20% amorphous silica (microfossils and tephra) for the biogenic ooze, and 30% calcite, 50% clay minerals and 20% lithics (quartz and plagioclase) for the silty clays (Supplementary Fig. 1). On average, the 50% clay mineral fraction contains 92% smectite (montmorillonite), 8% kaolinite and $<1\%$ illite¹⁶. It might be anticipated from previous work on smectite-rich sediments that the abundance of smectite would imply that the silty

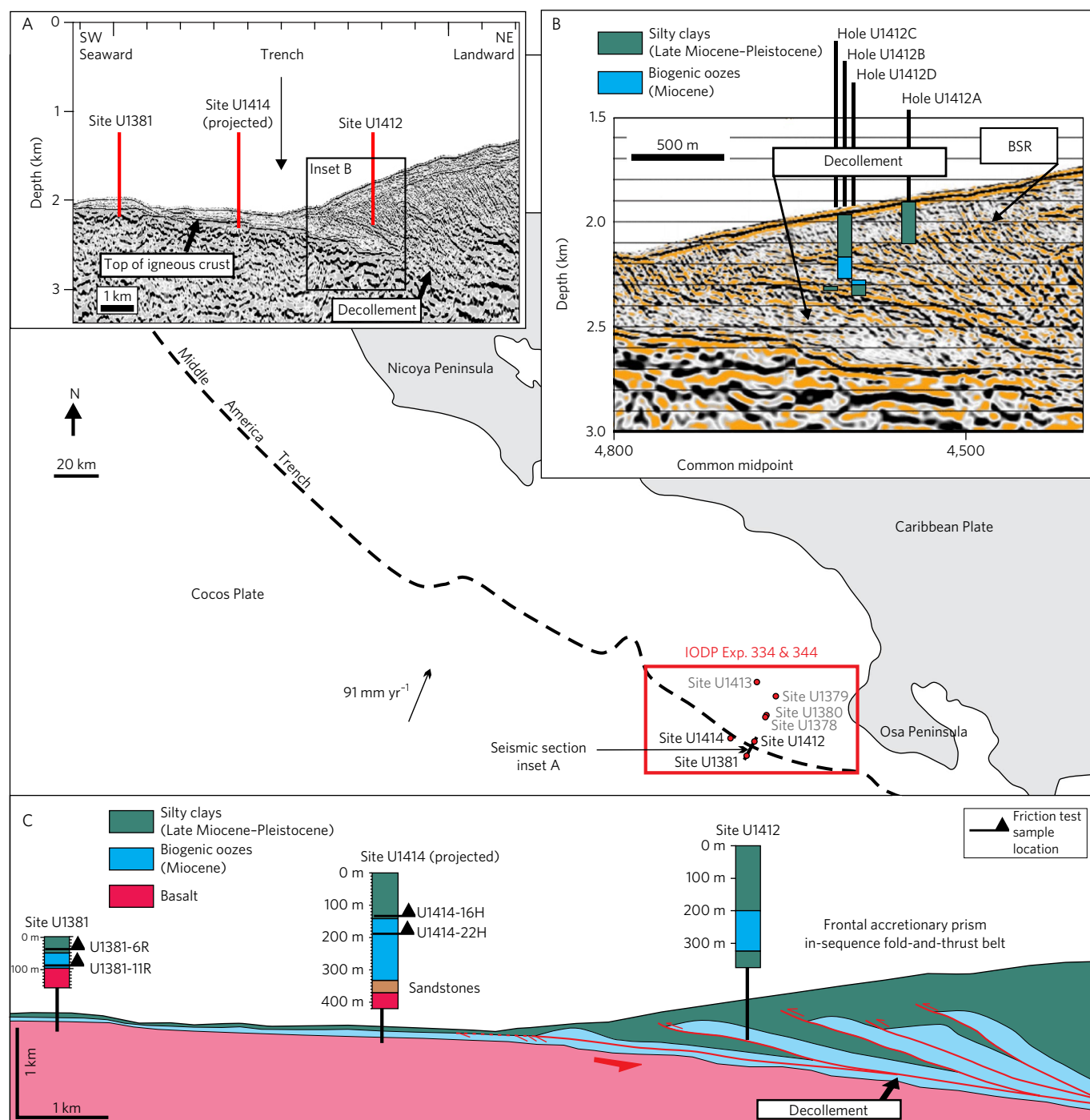


Fig. 2 | Location of ODP Leg 170 and IODP Exp. 334 and 344 (CRISP) offshore Central America. Inset A: Post-stack depth-migrated seismic section centred at the trench along the Site U1381/Site U1412 transect (detail of BGR99 Line 7)¹⁴. Inset B: Detail of the Site U1412 location and recovered material. Inset C: Stratigraphy of the drilled sites and conceptual cartoon of the accretionary system at the front of the CRISP transect as implied by the offshore drilling. The detachment layer is localized within the biogenic oozes. Note the lateral and downdip variation of the sediment thickness: in particular, the biogenic oozes are about 50 m at Site U1381, 180 m at Site U1414 and 120 m at Site U1412. Site U1414 is projected laterally from the position indicated in the location map, therefore its thickness in the cross-section is not the effective drilled thickness, which is reported in the log. The location of the samples used for the friction tests is also shown.

clays should be the weaker layer in this oceanic sedimentary succession^{8,17}. This stands in contrast with the geometric and drill evidence described above.

The presence of a frontal accretionary prism allows us to analyse the velocity-dependent frictional behaviour of incoming sediment, and apply this knowledge to infer the mechanical behaviour near the toe of the frontal prism built from these sediments (Fig. 2, inset B).

The CRISP setting is ideal to study the effect of slip velocity on sediments, because other factors that could cause their weakening, such as temperature and fluid–rock interactions, are negligible, in particular in biogenic oozes. At Site U1412, in situ temperature measurements linearly extrapolated to the depth of the old frontal megathrust estimate $T=40^{\circ}\text{C}$ (ref. ¹⁸), while thermal models imply $T<30^{\circ}\text{C}$ (ref. ¹⁷). Fluid overpressure can also weaken

sediments, as recently reported by experiments on material from the same Site U1414 (ref. 12). Both Site U1381 and Site U1414 show that biogenic oozes compact more slowly than silty clays. In particular, at Site 1414 the porosity of the oozes ($\approx 50\%$ on average) locally increases to $\approx 80\%$ at ≈ 225 mbsf, before decreasing to the base of the sediments. Fluid-rich sediment layers have also been identified by reflection seismics to be located between the basement and the basal decollement¹⁵. However CRISP drilling recorded no signs of fluid overpressure across the old frontal thrust as well as in the incoming plate sections. Pore fluids extracted from sediments adjacent to the old frontal megathrust have lower than seawater salinity¹⁸. At Site U1412, the increasing Ca^{2+} content in the pore fluids with depth indicates that no diagenesis other than compaction has begun within drilled sediments¹⁸. Dissolved CO_2 and hydrocarbons were measured only in the upper silty clay unit of Site U1412: the most abundant species is methane (0.65 vol%), while CO_2 is ~ 0.01 vol% (ref. 18). In the biogenic oozes, this value is likely to be higher; however, breakdown of organic matter and decarbonation of limestone are expected to occur only deeper than 60 km (refs 19,20).

Friction experiments in silty clays and biogenic oozes

To determine the mechanical behaviour of sediments under appropriate pressure–temperature conditions for the frontal prism, we conducted 23 experiments (Supplementary Information) using the rotary shear machine SHIVA (ref. 21). Incoming plate sediments from Site U1381 and Site U1414 were carefully powdered to a grain size $< 250 \mu\text{m}$ to preserve intact most of the microfossil tests. Samples were dried to a maximum T of 50°C for 12 h and rehydrated with distilled water to reproduce the relative moisture content of the original drill cores here expressed as a percentage of weight of water/weight of bulk sample (that is, 25 and 80 wt% water content for silty clays and 50 wt% water content for oozes)^{18,22}. Powders were also sheared under room-humidity conditions to provide a reference endmember. Experiments were all conducted at room temperature. Two-millimetre-thick layers of powders were confined within a ring-shaped (35–55 mm internal/external diameter) steel holder²³ and sheared under a constant normal stress $\sigma_n = 5$ MPa (equivalent to ~ 200 m depth) to reproduce shallow depth conditions. Fluid pressure can vary locally, due to the instantaneous frictional heating at seismic slip rates, although these pressure variations were not monitored. All mechanical results are therefore provided in terms of the recorded shear stress τ , which results in an effective friction coefficient $\mu^* = \tau / \sigma_n$, versus slip (D) and slip rate (V). All samples were initially sheared at $1 \times 10^{-5} \text{ m s}^{-1}$ for 10 mm to attain both compaction and the residual shear stress level (τ_0) to be used as the initial condition for the experiments (pre-shear phase) and arguably as a proxy for the state of shear stress preceding earthquake rupture at the trench. After this phase, a 300 s hold was set before applying a constant velocity for 1 m and 3 m of total displacement at 0.01 and 1 m s^{-1} , the latter being close to the slip velocity calculated for the 2011 $M_w 9$ Tōhoku-Oki earthquake²⁴, to the high-slip patches of tsunami earthquakes in Nicaragua and Peru^{25,26}, and to values from dynamic rupture simulations of near-trench seismic slip²⁷.

The residual shear stress (τ_0) recorded at the end of the pre-shear phase is well reproduced for the silty clays for all experiments, with standard deviations (s.d.) < 0.15 MPa. Biogenic oozes have the largest variations (Fig. 3a,b and Supplementary Information) with s.d. as large as 0.28 MPa (Fig. 3a,b). In general, reproducibility is worse in biogenic oozes than in silty clays. This may be caused by the heterogeneity of the biogenic material forming the oozes. In the pre-shear phase, both silty clays and oozes show slip-weakening and slip-strengthening behaviour (Fig. 3a,b). Wet oozes are overall stronger than wet silty clays, in agreement with previous observations for slip velocities $< 3 \times 10^{-4} \text{ m s}^{-1}$ (ref. 13).

At 0.01 m s^{-1} , water content plays a major role. Under room-humidity conditions and during the initial acceleration stage,

silty clays and biogenic oozes have a similar peak in shear stress ($\tau_p = 3.31 \pm 0.04$ MPa and $\tau_p = 3.27 \pm 0.33$ MPa, respectively) (Fig. 3a). With increasing slip, both materials have a slip-weakening behaviour within the first 0.05 m of slip, followed by slip-strengthening (Fig. 3a). In the presence of water, silty clays become clearly weaker than biogenic oozes. The frictional sliding behaviour of wet silty clays is quite reproducible, with an initial decay that becomes nearly slip-neutral to slightly slip-strengthening reaching a steady-state shear stress $\tau_{ss} = 0.83 \pm 0.02$ MPa at 25% wt H_2O . Biogenic oozes are slip-weakening over the entire duration of the experiment, but have an initial stage of abrupt weakening followed by a recovery stage during the first 0.02 m of slip before reaching $\tau_{ss} = 1.34 \pm 0.19$ MPa at 50% wt H_2O .

At 1 m s^{-1} and room-humidity conditions, all samples have initial slip-weakening behaviour (Fig. 3b) with a similar peak in shear stress ($\tau_p \sim 3.45$ MPa) after the initial acceleration stage. However, the shear stress decays faster in biogenic oozes than in silty clays and persists to a slightly higher steady-state value calculated at the end of each test ($\tau_{ss} = 2.22 \pm 0.26$ MPa for oozes versus $\tau_{ss} = 1.76 \pm 0.22$ MPa for silty clays). In the presence of water, the experiments on oozes show peaks of shear stress similar to those at room-humidity conditions with an average of $\tau_p = 3.41 \pm 0.33$ MPa, but present an abrupt weakening stage before reaching a steady-state value of $\tau_{ss} = 0.57 \pm 0.05$ MPa (Fig. 3b). The peak shear stress for silty clays is weaker ($\tau_p = 1.67 \pm 0.14$ MPa, 25% wt H_2O and $\tau_p = 1.45 \pm 0.04$ MPa, 80% wt H_2O), decay is characterized by a short (flash) initial weakening followed by a slow stage of strengthening before further reduction to the steady-state value ($\tau_{ss} = 0.68 \pm 0.06$ MPa, 25% wt H_2O and $\tau_{ss} = 0.56 \pm 0.01$ MPa, 80% wt H_2O).

The above experiments have shown that, during the onset of seismic slip rates (1 m s^{-1}), biogenic oozes are always slip-weakening. Importantly, at lower slip rates ($\leq 0.01 \text{ m s}^{-1}$), wet silty clays are weaker than oozes (Fig. 3a), and deformation would localize more easily by creeping within silty clays than within biogenic oozes, while the two fault materials become similarly weak at seismic slip rates (Fig. 3b).

Propagation of slip to the trench

However, sliding friction alone does not control the onset of slip during an earthquake. Indeed, an energy balance^{28,29} (Supplementary equation (1)) indicates that seismic rupture can occur when the elastic strain energy release E (which does increase with τ_0) equals or exceeds the summed dissipation of both fracture energy G_f (depending on τ_p and τ_{ss}) and sliding friction work W_f (depending on τ_{ss}). Any excess energy $E_r = E - (G_f + W_f)$ is then available for wave radiation, and under similar circumstances, faults with larger E_r are more likely to slip seismically. As noted above, biogenic oozes have a sharp slip-weakening behaviour while silty clays are slip-strengthening before decaying to steady state. Therefore, both the occurrence of strengthening in the silty clays and the stronger value of the residual shear stress (τ_0) in oozes are relevant factors to the propagation of slip.

Using τ_0 measured in the slow ($10 \mu\text{m s}^{-1}$) slip experiments (Supplementary Fig. 2) as a proxy of pre-seismic stress on the fault, we estimate values of the excess energy E_r from 23 experiments (Supplementary Table 1). At 0.01 m s^{-1} , E_r is similar for both silty clays and oozes (with the exception of one wet experiment in oozes, Fig. 3c), suggesting that slip can propagate easily in both types of sediment. However, at 1 m s^{-1} , wet oozes have a much higher residual stresses τ_0 than wet silty clays. Therefore, oozes are prone to larger strain energies E and capable of accumulating the elastic strain required to produce a ‘locked’ patch on a plate interface at shallow depths³⁰ (provided that the elastic strain is not released by adjacent weaker lithological units).

Recent experiments on material from the same Site U1414 suggest that at T between 70°C and 140°C and $P_f = 120$ MPa, subduction thrust earthquakes would preferentially nucleate in biogenic oozes instead of silty clays¹². If this is true, once rupture is initiated it could

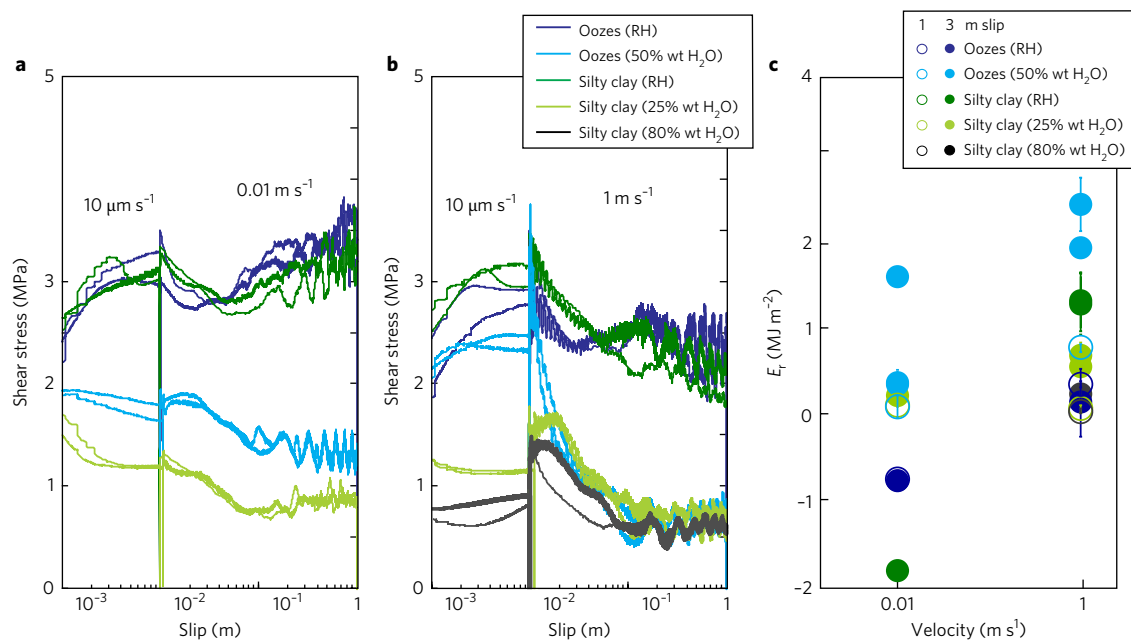


Fig. 3 | Summary of experimental results. Different colours refer to different water content (see legends). **a**, Example shear stress as a function of slip obtained for low-velocity (0.01 m s^{-1}) experiments for silty clays and biogenic oozes for different water content. The first 10 mm of slip are tested at $10 \mu\text{m s}^{-1}$. **b**, Example shear stress as a function of slip obtained for high-slip-velocity (1 m s^{-1}) experiments for silty clays and biogenic oozes. The first 10 mm of slip are tested at $10 \mu\text{m s}^{-1}$. At room humidity (RH), both silty clays and oozes show a slip-weakening behaviour, with comparable values of both peak and steady-state shear stress. Weakening, though, is very abrupt and pronounced for the oozes. Under wet conditions, the peak shear stress for the silty clays is lower than the oozes, but silty clays show an initial slip-strengthening behaviour. At steady-state conditions, the shear stress is very similar for both materials. **c**, Excess energy $E_e = E - (W_f + G_e)$ available for rupture propagation and wave radiation, calculated from the experimental data (see Supplementary Information). Open and filled circles refer to 1 m and 3 m of slip, respectively. The error is the standard deviation of the excess energy propagated from uncertainties of independent variables in Supplementary Equation 1 (Supplementary Table 1).

then propagate updip along the oozes, as documented from the drilling results. However, in southern Costa Rica, thermal modelling predicts that $T > 70^\circ\text{C}$ are to be expected only at distances $> 25 \text{ km}$ from the trench¹⁷, in a region where subduction erosion predominates³¹. Therefore, while the velocity-related friction behaviour of the oozes versus silty clays is relevant for the 5–10-km-wide frontal accretionary prism, at the depths of earthquake nucleation, the host material would be expected to be upper-plate rocks instead of these sediments.

Finally, laboratory-measured yield stresses for the oozes and silty clays are both easily exceeded in nature by the stress transient associated with fault propagation near the trench during a megathrust earthquake, as inferred by the stress-drop values of the 2011 M_w 9 Tohoku-Oki earthquake³² or the Peru and Nicaragua tsunami earthquakes (Fig. 1)^{26,33}.

These combined geological, geophysical and mechanical observations imply that the thrusts found in the forearc toe offshore southeast Costa Rica were active during transient high slip rates (that is, rates possible only during earthquake slip to the trench).

The geological and mechanical observations discussed in this paper imply that the subduction of biogenic oozes has the potential to create the conditions for earthquake slip to the trench that will greatly amplify the tsunami hazard in this and many other subduction systems, in particular along the Cocos and Nazca subduction zones (Fig. 1). Our observations indicate that biogenic oozes can provide a valuable record of past slip to the trench, and that past slip events can be effectively assessed locally by drilling into frontal prisms in high seismic and tsunami hazard areas.

Methods

Data availability. The drill core samples and data provided by the IODP are available from the LIMS Report database at <http://web.iodp.tamu.edu/LORE/> (request code: VANN). The experi-

mental data are available at <https://zenodo.org/record/1003549#.WesP7rVx200> and in the Supplementary Information. The seismic data are available from the authors on request.

Received: 25 April 2017; Accepted: 24 October 2017;

Published online: 27 November 2017

References

- Ito, Y. et al. Frontal wedge deformation near the source region of the 2011 Tohoku-Oki earthquake. *Geophys. Res. Lett.* **38**, L00G05 (2011).
- Fujiwara, T. et al. The 2011 Tohoku-Oki earthquake: displacement reaching the trench axis. *Science* **334**, 1240–1240 (2011).
- Satake, K., Fujii, Y., Harada, T. & Namegaya, Y. Time and space distribution of coseismic slip of the 2011 Tohoku earthquake as inferred from tsunami waveform data. *Bull. Seismol. Soc. Am.* **103**, 1473–1492 (2013).
- Wang, K. L. & Hu, Y. Accretionary prisms in subduction earthquake cycles: the theory of dynamic Coulomb wedge. *J. Geophys. Res.* **111**, B06410 (2006).
- Chester, F. M. et al. Structure and composition of the plate-boundary slip zone for the 2011 Tohoku-Oki earthquake. *Science* **342**, 1208–1211 (2013).
- Ikari, M. J., Kameda, J., Saffer, D. M. & Kopf, A. J. Strength characteristics of Japan Trench borehole samples in the high-slip region of the 2011 Tohoku-Oki earthquake. *Earth Planet. Sci. Lett.* **412**, 35–41 (2015).
- Faulkner, D. R., Mitchell, T. M., Behn, J., Hirose, T. & Shimamoto, T. Stuck in the mud? Earthquake nucleation and propagation through accretionary forearcs. *Geophys. Res. Lett.* **38**, L18303 (2011).
- Ujii, K. et al. Low coseismic shear stress on the Tohoku-Oki megathrust determined from laboratory experiments. *Science* **342**, 1211–1214 (2013).
- Moore, J. C., Plank, T. A., Chester, F. M., Polissar, P. J. & Savage, H. M. Sediment provenance and controls on slip propagation: Lessons learned from the 2011 Tohoku and other great earthquakes of the subducting northwest Pacific plate. *Geosphere* **11**, 533–541 (2015).
- Horn, D. R., Horn, B. M. & Delach, M. N. Sedimentary provinces of the North Pacific. *Geol. Soc. Am. Mem.* **126**, 1–22 (1970).
- Ikari, M. J., Niemeijer, A. R., Spiers, C. J., Kopf, A. J. & Saffer, D. M. Experimental evidence linking slip instability with seafloor lithology and topography at the Costa Rica convergent margin. *Geology* **41**, 891–894 (2013).

12. Kurzwaski, R. M., Stipp, M., Niemeijer, A. R., Spiers, C. J. & Behrmann, J. H. Earthquake nucleation in weak subducted carbonates. *Nat. Geosci.* **9**, 717–722 (2016).
13. Namiki, Y., Tsutsumi, A., Ujiie, K. & Kameda, J. Frictional properties of sediments entering the Costa Rica subduction zone offshore the Osa Peninsula: implication for fault slip in shallow subduction zones. *Earth, Planets and Space* <https://doi.org/10.1186/1880-5981-66-72> (2014).
14. Arroyo, I. G., Grevemeyer, I., Ranero, C. R. & von Huene, R. Interplate seismicity at the CRISP drilling site: The 2002 Mw 6.4 Osa Earthquake at the southeastern end of the Middle America Trench. *Geochem. Geophys. Geosyst.* **15**, 3035–3050 (2014).
15. Bangs, N. L., McIntosh, K. D., Silver, E. A., Kluesner, J. W. & Ranero, C. R. Fluid accumulation along the Costa Rica subduction thrust and development of the seismogenic zone. *J. Geophys. Res. Solid Earth* **120**, 67–86 (2015).
16. Charpentier, D. et al. Mineralogy and fluid content of sediments entering the Costa Rica subduction zone—results from Site U1414, IODP Expedition 344. In *AGU Fall 2013 Meeting abstr.* T34C-04 (American Geophysical Union, San Francisco, 2013).
17. Kameda, J. et al. Pelagic smectite as an important factor in tsunamigenic slip along the Japan Trench. *Geology* **43**, 155–158 (2015).
18. Harris, R. N. et al. In *Proc. IODP* Vol. 344 (IODP, Texas, 2013); <https://doi.org/10.2204/iodp.proc.344.101.2013>
19. Gorman, P. J., Kerrick, D. M. & Connolly, J. A. D. Modeling open system metamorphic decarbonation of subducting slabs. *Geochem. Geophys. Geosyst.* **7**, GC001125 (2006).
20. Kerrick, D. M. & Connolly, J. A. D. Metamorphic devolatilization of subducted marine sediments and the transport of volatiles into the Earth's mantle. *Nature* **411**, 293–296 (2001).
21. Di Toro, G. et al. From field geology to earthquake simulation: a new state-of-the-art tool to investigate rock friction during the seismic cycle (SHIVA). *Rendiconti Lincei* **21**, 95–114 (2010).
22. Vannucchi, P. et al. In *Proc. IODP* Vol. 334 (Integrated Ocean Drilling Program Management International, Inc., Tokyo, 2012); <https://doi.org/10.2204/iodp.proc.334.2012>
23. Smith, S. A. F. et al. Coseismic recrystallization during shallow earthquake slip. *Geology* **41**, 63–66 (2013).
24. Uchide, T. High-speed rupture in the first 20 s of the 2011 Tohoku earthquake, Japan. *Geophys. Res. Lett.* **40**, 2993–2997 (2013).
25. Piatanesi, A., Tinti, S. & Gavagni, I. The slip distribution of the 1992 Nicaragua earthquake from tsunami run-up data. *Geophys. Res. Lett.* **23**, 37–40 (1996).
26. Ihmle, P. F., Gomez, J.-M., Heinrich, P. & Guibourg, S. The 1996 Peru tsunamigenic earthquake: broadband source process. *Geophys. Res. Lett.* **25**, 2691–2694 (1998).
27. Hirono, T. et al. Near-trench slip potential of megaquakes evaluated from fault properties and conditions. *Sci. Rep.* **6**, 28184 (2016).
28. Andrews, D. J. Rupture velocity of plane strain shear cracks. *J. Geophys. Res.* **81**, 5679–5687 (1976).
29. Kanamori, H. & Rivera, L. in *Earthquakes: Radiated Energy and the Physics of Faulting* Vol. 170 (eds Abercrombie, R., McGarr, A., DiToro, G. & Kanamori, H.) 3–13 (Geophysical Monograph Series, American Geophysical Union, Washington DC, 2006).
30. LaFemina, P. et al. Fore-arc motion and Cocos Ridge collision in Central America. *Geochem. Geophys. Geosyst.* **10**, Q05S14 (2009).
31. Vannucchi, P. et al. Rapid pulses of uplift, subsidence, and subduction erosion offshore Central America: implications for building the rock record of convergent margins. *Geology* **41**, 995–998 (2013).
32. Brown, L., Wang, K. & Sun, T. Static stress drop in the Mw 9 Tohoku-oki earthquake: heterogeneous distribution and low average value. *Geophys. Res. Lett.* **42**, 10.595–10.600 (2015).
33. Satake, K. Mechanism of the 1992 Nicaragua tsunami earthquake. *Geophys. Res. Lett.* **21**, 2519–2522 (1994).

Acknowledgements

This research used samples and data provided by the International Ocean Drilling Program (IODP) (www.iodp.org/access-data-and-samples). The JOIDES Resolution crew and IODP technical team are thanked for their contributions during Exp. 334 and 344. P.V. acknowledges support during and following the expeditions from IODP-Italia, J-DESC and UK-IODP (Rapid Response Grant). E.S., S.A., S.N. and G.D.T. acknowledge the ERC CoG project 614705 'NOFEAR'. P.V. greatly benefited from discussions with J. Phipps Morgan. M. Stipp is thanked for constructive comments that significantly improved the paper. The data that support the findings of this study are available at <http://dx.doi.org/10.5281/zenodo.1003548>.

Author contributions

P.V. described the cores in ODP Leg 170 and Leg 205, and IODP Exp. 334 and Exp. 344, and sampled the sediments used for the experiments described in this paper, contributed to their interpretation and wrote the text. E.S. conducted the experiments and with the first author contributed to their interpretation, wrote the Supplementary Information and prepared the files for the data repository. S.A. conducted the experiments and contributed to their interpretation. K.U. and A.T. described the core in IODP Exp. 334 and performed an early set of experiments. G.D.T. and S.N. contributed to the interpretation of the experiments.

Competing interests

The authors declare no competing financial interests.

Additional information

Supplementary information is available for this paper at <https://doi.org/10.1038/s41561-017-0013-4>.

Reprints and permissions information is available at www.nature.com/reprints.

Correspondence and requests for materials should be addressed to P.V.

Publisher's note: Springer Nature remains neutral with regard to jurisdictional claims in published maps and institutional affiliations.